IN-SITU COMBINED SMALL- AND WIDE-ANGLE X-RAY SCATTERING FOR THE STUDY OF NANOPARTICLE DYNAMICS IN AN ETHYLENE DIFFUSION FLAME STABILIZED BY A METAL PLATE

L. Vallenhag*, S. E. Canton and F. Ossler***
linda.vallenhag@forbrf.lth.se
*Division of Combustion Physics, Lund University, Box 118, SE-221 00 Lund, Sweden
**MAX-lab, Lund University, Box 188, SE-221 00 Lund, Sweden

Abstract
Combined small- and wide-angle X-ray scattering techniques were used to study the dynamics of nanoparticle formation in-situ in an ethylene diffusion flame closely below a stabilizing and cooling metal plate on which particles condensed. The detectors allowed continuous monitoring of scattering intensities with a high dynamic range. The formation of species in the gas phase and during transfer into the condensed phase was studied as the temperature inside the flame decreased. Measurements were performed at two different heights above the burner monitoring X-ray scattering intensities and temperatures at the burner surface, at medium flame height and at the cooling plate. Strong changes were observed in the scattering properties as the temperatures decreased with time. The SAXS results show that a large number of particles between 1 and 10 nanometers are produced as the local temperature is decreased. The results have important implications on combustion control and the release of small nanoparticles.

Introduction
The physical and chemical mechanisms leading to particle formation during combustion are still to a great deal unknown and much effort is being invested in increasing the understanding [1]. Combustion generated particles are of a major concern from the environmental, health and fuel economy perspective. Particles can also play an important role for the efficiency of heat transfer, overall efficiency in complex combustion systems, and production of nanostructured materials. All these different applications require an accurate knowledge on how to control particle formation and dynamics. To be able to study the particle formation process in combustion, non-intrusive *in-situ* techniques are necessary not to affect the temperature, species composition and flow fields that strongly influence the dynamics. Laser techniques that can be used to characterize nanoparticles *in-situ* are based on laser scattering/extinction [2] (LSE) and laser-induced incandescence [3]-[4] LII. However, it is difficult to get information about the size distribution function and particle structure with these techniques. Radiation with wavelengths on the order of the length of the interatomic bond distances should be used in order to resolve the structure and the size of nanoparticles. This bond distance is typically 1–2 Å, which correspond to radiation in the hard X-ray region.

Synchrotron X-ray scattering techniques are used to characterize nanoparticles *in-situ*: small-angle X-ray scattering (SAXS) and wide-angle X-ray scattering (WAXS) have been used to characterize the size distribution of soot particles [5]-[11] and to study the sub-nanometer structure [12]-[13], respectively. These scattering techniques analyze the scattered intensity as a function of the exchange in momentum, q, between the incident photon and the target

$$q = \frac{4\pi}{\lambda}\sin(\theta/2) \quad (1)$$

where λ is the wavelength of the incident photon and θ is the scattering angle.

In this work we show results from our combined SAXS and WAXS studies on the dynamics of soot formation in a diffusion-based ethylene flame stabilized by a metal plate and operating at atmospheric pressure condition. The dynamics of particle generation for length scales between 3 Å and 200 Å was investigated slightly below the plate for two different heights. The scattering measurements were supported by synchronous temperature readings during the experimental runs.

Experiments

The experiments were performed at beamline D611 at MAX-lab, Lund, Sweden. The photon flux was 10^{12} photons s^{-1} with a beam size of approximately 1 x 2 mm^2 (vertical x horizontal). A monochromator with two planar multilayer mirrors gave a relative bandwidth $\Delta\lambda/\lambda$ of approximately 0.01. Photon energies from 5 to 8 keV (λ = 1.55–2.48 Å) were used. The main parts of the experimental set-up can be seen in Fig. 1. The X-ray beam was passed through a pinhole in order to narrow the beam size. A detector scintillator combined with a photomultiplier tube (PMT) was placed perpendicular to the X-ray beam to measure air-scattered photons with an intensity proportional to the incident X-ray radiation. The burner was a non-cooled porous bronze plug with a diameter of 2 cm with ethylene burning as a diffusion flame. Between 1 cm and 2 cm above the burner was a metal plate placed, working as a flame stabilizer and cooling support for the soot to grow on. Another purpose with the metal plate was to stimulate the condensation of soot precursors and particles in the gas phase. The X-ray beam passed close to 1 mm below the plate and the scattered radiation from the soot particles in the flame was collected by the SAXS and the WAXS detectors. Three thermocouples, TC_1-TC_3, were placed at strategic positions: close to the burner, at medium height and close to the metal plate, respectively.

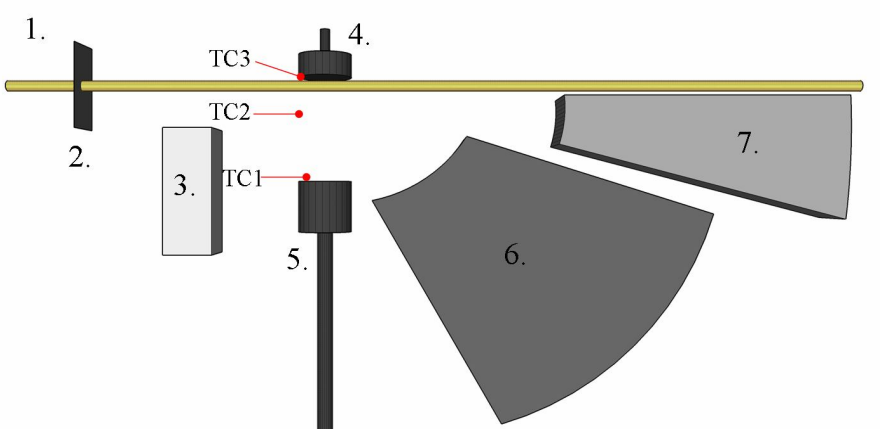

Figure 1. The experimental set-up for flame measurements. (1) X-ray beam, (2) pinhole, (3) reference PMT, (4) metal plate, (5) burner, (6) WAXS detector (7) SAXS detector and (TC_1-TC_3) three thermocouples.

The SAXS detector consisted of 20 channels evenly distributed over a range from 0.5° to 10° and the WAXS [12]-[14] existed of 6 channels from 17.5° to 60°. The scattered radiation from every channel was registered by a scintillator/PMT detection unit. The channel output was sent to a trans-impedance amplifier before arriving to an A/D sampler allowing a maximum sampling rate of 204.8 k sample s^{-1} corresponding to a time resolution close to

5 μs. The distance from the front end to the measuring area was 150 mm for the SAXS detector and 50 mm for the WAXS detector. The data acquisition and the processing of the sampled signals were computer controlled with LabVIEW and the data were sampled synchronously and continuously on all channels without processing dead time. Based on previous work [13]-[14] the scattered intensity I_i at channel i can be described by equation (2),

$$I_i(t, q(\lambda,\theta), \theta, \varphi) = I_0 c_i r_e^2 p(\theta,\varphi) N(t) \sum_{j=1}^{M} x_j(t) \left[\frac{d\sigma_{sj}(q_i)}{d\Omega} \right] \Delta\Omega_i \Delta V_i \quad i = 1, \ldots, n \tag{2}$$

where I_0 is the irradiance of the source, n is the number of channels, t is the time of the measurement, θ is the scattering angle and φ is the angle between the scattering plane and the plane of polarization, which is 90° in these synchrotron-based experiments. c_i is the calibration factor for channel i, r_e is the electron radius, N is the total concentration of species, x_j is the mole fraction of species j and $\frac{d\sigma_{sj}(q_i)}{d\Omega}$ is its differential scattering cross section. For $\varphi=90°$ is $p(\theta,\varphi)=1$, ΔV_i is the measured volume and $\Delta\Omega_i$ is the solid angle, respectively, of channel i.

The signals were continuously sampled without dead time and to increase the signal-to-noise ratio the data were processed using two alternative averaging procedures, referred to as Averaging (AV) and On Line Background Subtraction (OLBS) averaging. AV was used by turning periodically on and off the X-ray beam so that the background could be subtracted after the experimental run. Instead the OLBS allowed background reduction and averaging directly on-line before storing data on the computer. A chopper modulated the radiation at a frequency typically set between 1 kHz and 2 kHz and a special software was then used to process the data and do the averaging on-line before storing it on the computer.

The experimental set-up was calibrated by comparing the measured scattering signals on air with theoretical calculations. Another more direct way to observe changes in the scattering, not requiring calibration factors was to plot the ratio γ defined by the following equation

$$\gamma_i(q_i, t) = \frac{I_i(q_i, t)}{I_i(q_i, t_0)} \quad i = 1, \ldots, n \tag{3}$$

where t_0 is the starting time and n is the number of channels. This way of representing data is preferably when changes relative the initial conditions are significant.

The experiments were performed at two different heights in the flame (12 mm and 17 mm) with an ethylene flow of 0.23 litre min^{-1} (velocity 1.2 cm s^{-1}) using flow controllers. The measurements were done in time spans of approximately 1–2 hours. The metal cooling plate was taken off and cleaned before each run.

Results and Discussion

Figure 2 shows the results from 12 mm height above the burner (HAB) for seven different times during a 90 minutes experimental run. Figure 2a) shows the scattering intensity as a function of the exchange momentum and Fig. 2b) shows the corresponding γ data. In order to directly see the length scales involved in the scattering, the characteristic length scale $L=2\pi/q$ has been inserted as the upper x-axis. The scattering intensities in the graphs were averaged over 50 s. The temperatures (T_1-T_3) given by the thermocouples TC_1-TC_3 are plotted in Fig. 2c) evidencing the times for the corresponding scattering data reported in a) and b). TC_1 was placed 1 mm above the burner surface and that temperature was stable around 800 K, but

the temperatures T_2 and T_3 started at 1000 K and then constantly decreased probably mostly due to soot growing on the thermocouples. Interesting to note is that T_3 shows the strongest decrease with time and that two crossing points, with T_2 and T_1, respectively seem to be closely related to break points in the scattering dynamics. We will call these A and B. The corresponding temperatures T_A = 878 K and T_B = 770 K were obtained at 1499 s and at 4300 s, respectively. The temperature continued to decrease until it reached a minimum at 750 K after 5000 s.

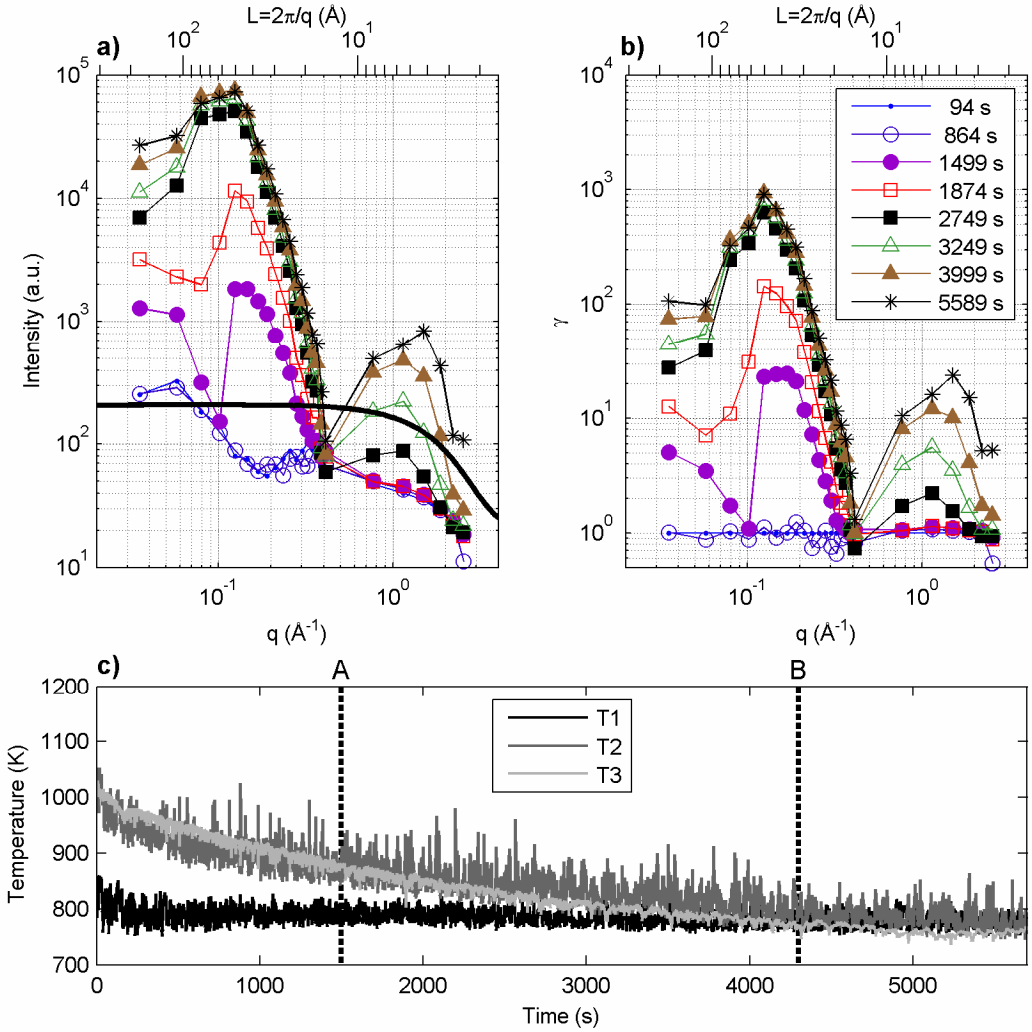

Figure 2. Experimental run at 5 keV (λ = 2.48 Å) at 12 mm height above the burner. a) Shows the scattering intensity for different times and the theoretical scattering for air (black line). b) Shows the corresponding γ ratio. The characteristic length scale ($L=2\pi/q$) can be seen as the upper x-axis. c) The temperature (T_1-T_3) from three thermocouples (TC_1-TC_3) placed at 1 mm above burner surface, at medium height and at plate.

Figure 2a) shows initially pure gas-phase scattering. The SAXS scattering was stronger than for air for $q < 0.1$ Å^{-1}. This scattering was caused by soot particles and particles originating from the outer diffusion region of the flame. During the first 864 s the scattering pattern did not change significantly. Then first break point in the scattering properties was observed close to the first crossing point A at 1499 s. The intensity in the region 0.1 Å^{-1} < q < 0.4 Å^{-1} showed a strong increase and a minimum appeared clearly for 0.4 Å^{-1} < q < 0.7 Å^{-1} and did not seem to change in intensity with time. Up to 1874 s the SAXS increased while WAXS remained almost unchanged. The second break point was observed between 1874 s and 2749 s when both the SAXS and WAXS signals increased strongly and a maximum in the

WAXS close to 1 $Å^{-1}$ was developed. Between 2749 s and 3999 s there were only very weak changes for 0.1 $Å^{-1}$ < q < 0.4 $Å^{-1}$ and only the SAXS for smallest and the WAXS at the higher q values increased considerably. A third break point was observed between 3999 s and 5589 s not far from the second crossover, B of T_3, when the WAXS developed a graphitic like structure (q close to 1.75 $Å^{-1}$).

Results from 17 mm HAB experiments can be seen in Fig. 3 where a) and b) show the scattering intensity and the ratio γ, respectively, and c) displays the temperature from the three thermocouples. There are more oscillations in the temperature curve given by TC_3 for the 17 mm HAB than for 12 mm HAB experimental run. This was due to a more unsteady flame higher above the burner. TC_1 was placed at the surface, which explains why there is an increase in the temperature the first 1000 s compared to the 12 mm HAB results where the thermocouple was placed 1 mm above the burner. The 17 mm experiment showed faster dynamics and the entire experiment was performed in 3000 s. The temperature and times cross over points A and B were T_A = 906 K and T_B = 810 K at 885 s and 1900 s, respectively.

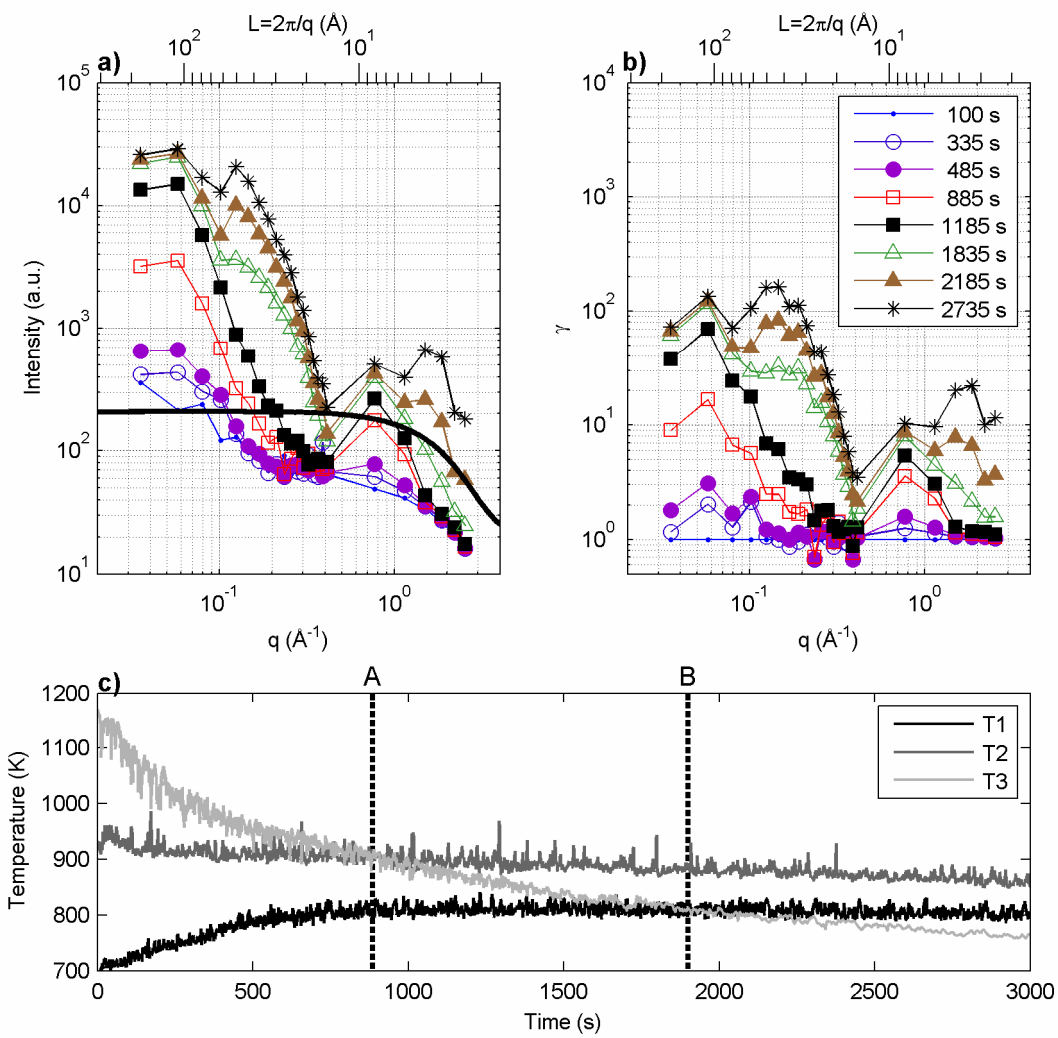

Figure 3. Experimental run at 5 keV (λ = 2.48 Å) at 17 mm height above the burner. a) Shows the scattering intensity for different times and the theoretical scattering for air (black line). b) Shows the corresponding γ ratio. c) The temperature from three thermocouples (TC_1-TC_3) placed at the burner surface, at the cooling plate and in between.

During the first 1000 s both SAXS and WAXS increased as the burner surface temperature increased, speeding up the chemistry and soot production yielding higher concentrations of nanoparticles. The first breakpoint appeared at 1835 s when the scattering in the region 0.1 $Å^{-1}$ < q < 0.4 $Å^{-1}$ increased with time, after the plate temperature decreased below the middle position temperature. A local WAXS maximum can be observed in the region 0.4 $Å^{-1}$ < q < 1.0 $Å^{-1}$, i.e. for smaller values than for the 12 mm HAB flame. This may indicate that larger structures were formed than correspondingly for the 12 mm HAB case. The intensity at the minimum between 0.4 $Å^{-1}$ and 0.7 $Å^{-1}$ was not constant as for the previous experiment, but increased noticeably with time. A second and last breakpoint in the scattering dynamics occurred between 1835 s and 2185 s close to the second crossover B of T_3. The SAXS in the smallest q region hardly changed while the scattering between 0.1 and 0.4 $Å^{-1}$ increased. At the same time the graphitic structure appeared and increased in intensity.

Interesting to note in these investigations is the appearance of scattering features between 0.1 and 0.4 $Å^{-1}$, which correspond to length scales between 63 Å and 16 Å and appear before the graphitic structures observed in the WAXS region. The nature of these particles is not yet identified but could be attributed to condensing species forming clusters or droplet-like structures as the local temperature decreases. The shape of the scattering curve shows initially distinctly two minima close to 0.1 $Å^{-1}$ and between 0.4 $Å^{-1}$ and 0.7 $Å^{-1}$. The position of the first minimum shifts to lower q values and corresponds to an increase of the size of these species. In relation to spherical particles that is consistent with an increase of the diameter. The intensity of the minimum decreases with time is also consistent with a droplet system becoming more polydisperse. The WAXS and the second minimum between 0.4 and 0.7 $Å^{-1}$ agree with results previously published [14].

Due to the potentially very hazardous nature of these small nanoparticles more investigations directed towards classifying the chemical properties of these species are needed. The detection system will be upgraded to include more detections channels in particular for the region between 0.4 $Å^{-1}$ and 1 $Å^{-1}$ and to increase the resolution in the WAXS region in order to obtain more information on the nanometer and sub-nanometer scale structure. Sampling techniques will also be employed in order to test the species with complementary diagnostics tools.

Conclusions

Combined SAXS and WAXS measurements of particle formation dynamics have been performed for two flame systems. The results have interesting implications to combustion. A large number of particles with a length scale below 10 nm are produced in fuel rich flames when the flame temperature is lowered. Consequently local flame quenching, e.g. in unsteady and turbulent flames may produce very large amounts of small nanoparticles that are potentially dangerous for human health and the environment.

Acknowledgement

We acknowledge the support by Lennart Österman for the construction and implementation of the electronic amplification of the detection system, Peter Sondhauss for the finalization of the SAXS detector and beamline support. We also acknowledge The Swedish Energy Agency, the Swedish Research Council and the Center for Combustion Science and Technology (CECOST) for the financial support. We also thank the Crafoord Foundation for funds supporting the construction of our detectors.

References

[1] Bockhorn, H., D'Anna, A., Sarofim, A.F., Wang, H., Editors, *Combustion Generated Fine Carbonaceous Particles*, KIT Scientific Publishing, 2009

[2] Sgro, L.A., Minutolo, P., Basile, G., D'Alessio, A., "UV-visible spectroscopy of organic carbon particulate sampled from ethylene/air flames", *Chemosphere* 42: 671-680 (2001)
[3] Melton, L.A., *Soot diagnostics based on laser heating*, Appl. Opt. 23: 2201 (1984)
[4] Will, S., Schraml, S., Bader, K., Leipertz, A., "Performance characteristics of soot primary particle size measurements by time-resolved laser-induced incandescence", *Appl. Opt.* 37:5647 (1998)
[5] England, W.A., "An in situ X-ray small angle scattering study of soot morphology in flames", *Combust. Sci. and Tech.* 46: 83-93 (1986)
[6] Hessler, J.P., Seifert, S., Winans, R.E., "Spatially resolved small-angle X-ray scattering studies of soot inception and growth", *Proc. Combust. Inst.* 29: 2743-2748 (2002)
[7] Hessler, J.P., Seifert, S., Winans, R.E., Fletcher, T.H., "Small-angle X-ray studies of soot inception and growth", *Faraday Discuss*. 119: 395-407 (2001)
[8] di Stasio, S., Mitchell, J.B.A., LeGarrec, J.L., Biennier, L., Wulff, M., "Synchrotron SAXS (in situ) identification of three different size modes for soot nanoparticles in a diffusion flame", *Carbon*. 44: 1267-1279 (2006)
[9] Mitchell, J.B.A., Courbe, J., Florescu-Mitchell, A.I., di Stasio, S., Weiss, T., "Demonstration of soot particle resizing in an ethylene flame by small-angle X-ray scattering", *J. Appl. Phys*. 100: 124918 (2006)
[10] Sztucki, M., Narayanan, T., Beaucage, G., "In situ study of aggregation of soot particles in an acetylene flame by small-angle X-ray scattering", *J. Appl. Phys.* 101: 114304 (2007)
[11] Beaucage, G., Kammler, H.K., Mueller, R., Strobel, R., Agashe, N., Pratsinis, S.E., Narayanan, T., "Probing the dynamics of nanoparticle growth in a flame using synchrotron radiation", *Nat. Mater.* 3:370 (2004)
[12] Ossler, F. Larsson, J., "Exploring the formation of carbon-based molecules, clusters and particles by in situ detection of scattered X-ray radiation", *Chem. Phys. Let.* 387: 367-371 (2004)
[13] Ossler, F., Larsson, J., "Measurements of the structures of nanoparticles in flames by in situ detection of scattered X-ray radiation", *J. Appl. Phys.* 98: 114317 (2005)
[14] Ossler, F., Canton, S.E., Larsson, J., "X-ray scattering studies of the generation of carbon nanoparticles in flames and their transition from gas phase to condensed phase", *Carbon* 47: 3498-3507 (2009)